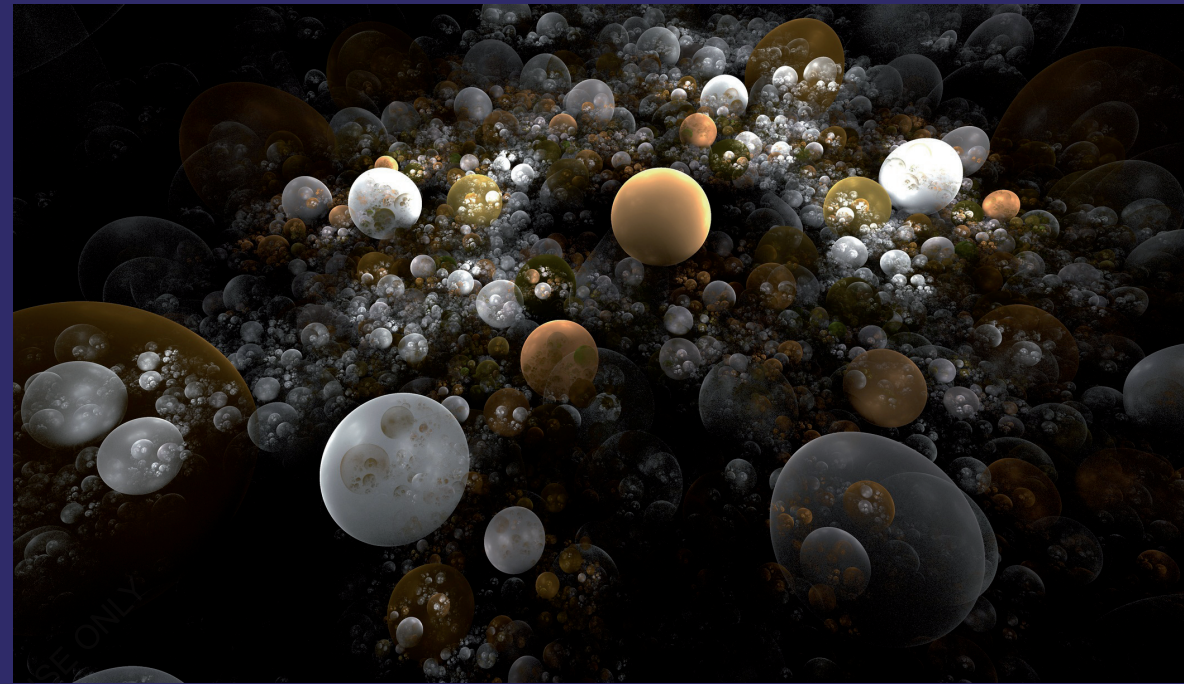


This book deals with the confined energy of a two electron in a spherical quantum dot. The interaction energy and its effect on confined energy are also been discussed. The singlet and triplet state of electron also analyzed. The external perturbation effects on hydrostatic pressure and temperature are also been studied. One can get the idea of finding energy of two electron quantum using perturbation method.

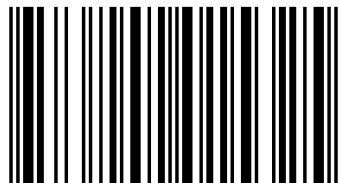


A. Rejo Jeice

Confined Energy Of Two Electrons In a Spherical Quantum dot



A. Rejo Jeice has authored or Co-authored more than 17 research papers in Quantum Mechanics. He has 10 years of teaching and research experience. His recent research focuses on Nanostructures and Quantum devices. At present he is working as Assistant Professor in Physics, in Annai Velankanni College, Thalayavattam, TamilNadu, India.



978-620-2-01532-5

 **LAMBERT**
Academic Publishing

A. Rejo Jeice

Confined Energy Of Two Electrons In a Spherical Quantum dot

FOR AUTHOR USE ONLY

FOR AUTHOR USE ONLY

A. Rejo Jeice

**Confined Energy Of Two Electrons In
a Spherical Quantum dot**

FOR AUTHOR USE ONLY

LAP LAMBERT Academic Publishing

Imprint

Any brand names and product names mentioned in this book are subject to trademark, brand or patent protection and are trademarks or registered trademarks of their respective holders. The use of brand names, product names, common names, trade names, product descriptions etc. even without a particular marking in this work is in no way to be construed to mean that such names may be regarded as unrestricted in respect of trademark and brand protection legislation and could thus be used by anyone.

Cover image: www.ingimage.com

Publisher:

LAP LAMBERT Academic Publishing

is a trademark of

International Book Market Service Ltd., member of OmniScriptum Publishing Group

17 Meldrum Street, Beau Bassin 71504, Mauritius

Printed at: see last page

ISBN: 978-620-2-01532-5

Copyright © A. Rejo Jeice

Copyright © 2017 International Book Market Service Ltd., member of OmniScriptum Publishing Group

All rights reserved. Beau-Bassin 2017

FOR AUTHOR USE ONLY

TABLE OF CONTENTS:

Abstract	1
1. 1 Introduction	2
1. 2 Methods and Calculations	9
1. 3 Results and Discussion	19
1. 4 Conclusion	37
References	39

FOR AUTHOR USE ONLY

FOR AUTHOR USE ONLY

CONFINED ENERGY OF TWO ELECTRONS IN A SPHERICAL QUANTUM DOT AND THEIR CORRELATION EFFECTS WITH EXTERNAL PERTURBATIONS

A. Rejo Jeice*

* Department of Physics, Annai Velankanni College, Tholayavattam,
kanyakumari dist -Tamil Nadu, India – 629157
rejojeice@gmail.com

Abstract

In the present chapter the confined energy of two electrons in a spherical QD and its interaction effects with external perturbations are investigated. The perturbation method is used to find the confined energy and interaction energy. The combined effect of hydrostatic pressure and temperature on interaction energy in a triplet state of two electron spherical quantum dot is computed. All the calculations have been carried out with finite models. The confined energy and its interaction effects of singlet and triplet state of GaAs/GaxIn1-xSb are discussed. A brief introduction about quantum dot also been given.

Key Words: Spherical quantum dot. Square well confinement. Correlation energies. Singlet and Triplet states. Total Confined energies

*E-mail address: rejojeice@gmail.com.

Phone. No: 08807841121

1.1 Introduction

The advancement of Science and Technology has created an overwhelming stream of opportunities for improving the quality of human life. Hence, the present chapter has been focused on probing certain key issues, like tuning of band gap by applying the external perturbations. GaAs/GaAlAs nanostructure has attracted much interest because of their broad range of applications in electronics, sensors, transducers, single electron transistors, quantum computers, solar cells and biomedical sciences. Due to the vast application of GaAs/GaAlAs material made as to motivate the study of correlation effects of two electron systems. The interest in transition property of the material made to study the singlet and triplet state energies of the system. The non-availability of the external perturbations like pressure and temperature on triplet state of two electrons quantum dot made to calculate the effects on it.

The development of Low Dimensional Semiconductor System (LDSS) has found the ample of applications in the field of nanoscience. In recent years, the study of LDSS and nanocrystals has been of a great interest in both the experimental and theoretical point of view. Hence the material scientist's focuses to fabricate the devices using LDSS such as the quasi quantum well (QW), quantum wire and quantum dot (QD) [1]. In the LDSS the energies of a

carrier, phonon and electron-phonon interactions are enhanced when the dimension of the physical system is reduced to nanometer scale which results entirely new characteristics.

1.1.1 Quantum Dot

In a QD or an artificial atom, there are discrete electronic energy levels, as in a molecule or atom, but in this case, the spacing of the electronic energy levels can be very precisely chosen by the experimenter through variation of the size. Hence the quantum dots (QDs) are fascinating one for the investigations in the Physics laboratory QDs with their own distinct characteristics, which has many similarities to the real periodic table. The development of methods to produce colloidal QDs in solution led to an explosive growth in research on these materials since, the new concepts of artificial solid could find use in wider range of applications. The three-dimensional confinement of electrons and holes drastically changes the electronic structure in QDs from that of bulk crystals with a continuous energy spectrum to that with essentially discrete energy levels. This is called a quantum size effect.

QDs are devices in which charge carriers are confined in all the dimensions. They are very interesting in optoelectronic properties and magnetic devices due to their singular nature of density of electrons. It is

possible to fabricate QDs containing a number of electrons with recent advances in nanofabrication technology. A perceptible nature of the impurity states in semiconductor QDs is one of the crucial problems in semiconductor Physics because impurities can dramatically alter the properties and performance of the quantum devices. In these quasi zero dimensional systems, the motion of the carrier is restricted to a narrow region of a few nanometer in dimension, the correlation among the electrons are shown appreciable.

In past few years, QDs have attracted considerable interest because of their atom-like properties make them a good venue for studying the Physics of confined carriers and many body effects. They could also lead to novel applications in memory chips, quantum computing and quantum cryptography and so on. In the artificial atoms of the QD analogy should not be carried too far. Unlike electrons in an isolated atom, carrier in semiconductor QDs (which contains a few thousand to tens of thousands of atoms arranged in a nearly defect-free three dimensional crystal lattice) interact strongly with lattice vibrations and could be strongly influenced by surface, defect or interface states.

One of the most important consequences of strong carrier confinement in QDs is the prominent role of many-body effects. Some of the many body effects have already been investigated in lithographically defined QDs,

including the Physics of Coulomb charging and Kondo effect. Coulomb interactions between the carriers control the quantum charging and carrier recombination dynamics in QDs. Measurements of transport properties in a magnetic field have been used for the filling of energy levels and the validity of Hund's rule in these electrostatically defined QDs. Unexpected effects have been reported in these systems, including the pair wise loading of electronics into QDs.

Self-assembled QDs are of great interest due to their application in optoelectronic devices. Two semiconducting materials with lattice mismatch of 5% is needed for the formation of the self-assembled QD by Stranski-Krastanow growth mode. InAs/GaAs and InAlAs/AlGaAs is characterized by Type - I structure where both the electrons and holes are located inside the dots. But in type - II QDs the QD forms an antidote for one of the types of carriers, e.g. holes in InP/GaInP system or the electrons in GaSb/GaAs. In the strongly optically populated type - II QDs, photoluminescence studies at high magnetic fields show the Landau level formation and also the type-II QD, the electron is confined in the dot and the hole is located in the barrier material. Transition from type - I to type - II is induced by changing the confinement potential.

Recently, high spatial and resolution techniques have been used to isolate the single dots and made it possible to remove the inhomogeneous broadening in non-linear spectra. These advances allow one to study the various physical phenomena such as

Fine structure splitting

Atomic - like excitation spectrum

Many body interactions

Dot - dot coupling

Origin of the line width

Bi - excitonic states

Zeeman splitting and diamagnetic shift and

Metal insulator transition

Amidst the mentioned LDSS, semiconductor QD is an excellent one to explore such remarkable confinement effects. The fabrication of these semiconductor QD in quasi zero dimensions shows exotic electron behavior due to electronic confinement. Since the energy levels of the confined electron in a QD are discrete as in an atom the QD is called as artificial atoms. The energy levels of the QD are 1s, 1p, 1d, 2s, etc.,. In the artificial atoms, electrons possess not only the charge but also a spin. The interplay of such properties of an electron incorporated with the confinement effect is

scientifically and technologically importance. The exploitation of the spin properties of an electron have attracted the researcher's towards the area of spintronics.

The correlation effects lead to an interesting phenomenon like Coulomb blockade, which is exploited in single electron transistors. Considerable efforts have been made on the estimation of correlation effect of few electrons in QD. The confinement will affect due to correlation energy (CE) and hence the study of correlation effects is included in the confined energy. The correlation effects are treated to various degrees of theoretical sophistication by several authors [2, 3]. The CE (electron-electron coulomb interaction energy) plays a vital role in varying the physical properties of LDSS such as optical, electronic, spintronics and transport phenomena. Transport and optical spectroscopy have revealed the field-tunable rich phases in few electron QD systems. Hence, it is important to calculate the low-lying states in the presence of confinement and electron-electron correlation. The electron-electron interaction effects include the mutual coulomb term. Hence the interaction in a QD becomes an interesting. Generally CE of an electronic system is defined as the difference between the exact energy and its Hartee-Fock energy in many body systems. Herein, it is described as the electron-electron interaction energy. The system is confined with the dot even in the absence of any other

attractive potential like columbic potential as in hydrogen atom is called confined energy. Also, the CE and total confined energy for the singlet and triplet state of spherical quantum dot (SQD) are studied.

In the quasi-zero dimensional systems the carrier motion is arrested to a narrow region with the dimension of a few nanometers and hence the correlation effects among the electrons are appreciable. Most of the calculations are infinite models with square well potential confinement or parabolic confinement. Reports on the finite barrier confinement with square well confinement are sparse. Unlike certain calculations which involved the extensible numerical work, closed analytical expressions have been obtained by treating electron correlations by perturbation method, which utilizes the evaluation of certain integrals by the mean value theorem. The effect of quantum confinement and electron-electron correlation has been reported for Si-deformed wires [4-5]. Light absorption, electron - hole pair dissociation and charge collection are considered to be the three key processes that control the overall power conversion efficiency of organic photovoltaic devices. Matching the electron hole pair diffusion length with the respective optical absorption length is a challenge for achieving high power conversion efficiencies in solar cells. In this context, the photogenerated singlet electron hole pair exhibit very short lifetimes because of their dipole-allowed spin radioactive decay, and

consequently, they have short diffusion lengths. In contrast, the radioactive decay of triplet electron hole pair is dipole forbidden; therefore, their lifetimes are considerably longer. Recent relevance in quantum information processing opens the system to manipulate singlet-triplet transition in the electrostatic gates and it is operated as qubits. These interesting phenomena have motivated to study the triplet state of LDSS. In the present chapter, the CE is calculated for GaAs embedded $\text{Ga}_x\text{In}_{1-x}\text{Sb}$ for the first time.

1.1.2 Objectives

The core objectives of the present chapter are:

- i) To find the confined energy of two electrons on a GaAs/ $\text{Ga}_x\text{In}_{1-x}\text{Sb}$ for the singlet and triplet state with correlation effects.
- ii) To study the effect of external perturbations such as pressure and temperature on CE in the triplet state of GaAs/ $\text{Ga}_{1-x}\text{Al}_x\text{As}$.

1.2 Methods and Calculations

1.2.1 Single Electron in a Spherical Quantum Dot

A single electron in a SQD is considered in the finite barrier model. In the absence of impurity, within the effective mass approximation, the Hamiltonian is given by,

$$H_1 = -\frac{\hbar^2}{2m^*}\nabla^2 + V_D(\mathbf{r}) \quad (1.1)$$

where m^* is the effective mass of the electron at the conduction band minimum, which is $0.067 m_0$ for GaAs [6], where m_0 is the free electron mass. In numerical calculations, the atomic unit is used in which $m_0 = e^2 = \hbar^2 = 1$. The confining potential $V_D(\vec{r})$ is given by,

$$V_D(\vec{r}) = \begin{cases} 0 & r \leq R \\ V_0 & r \geq R \end{cases} \quad (1.2)$$

where $V_0 = Q_c \Delta E_g(x)$ is the barrier height, Q_c is the conduction band offset parameter which is taken to be 0.658 [7]. Here, the band gap difference depends on the concentration of gallium. In the present case $\text{Ga}_x\text{In}_{1-x}\text{Sb}$ is the barrier medium in which GaAs dot is embedded. The total energy difference [8] between the dot and barrier media as a function of x , is given by

$$\Delta E_g(x) = 0.235 + 1.653x + 0.413x^2 \text{ eV} \quad (1.3)$$

Herein, $x = 0.1, 0.2$ and 0.3 and the value of V_0 turns to be 266.12, 383.03 and 505.39 meV respectively. Two lowest lying bound states are given by,

$$\Psi_{1s}(\vec{r}) = \begin{cases} N_1 \frac{\sin(\alpha_1 r)}{\alpha_1 r} & r \leq R \\ A_1 \frac{e^{-\beta_1 r}}{\beta_1 r} & r \geq R \end{cases} \quad (1.4)$$

$$\Psi_{1p}(\vec{r}) = \begin{cases} N_2 \left[\frac{\sin(\alpha_2 r)}{(\alpha_2 r)^2} - \frac{\cos(\alpha_2 r)}{(\alpha_2 r)} \right] \cos\theta & r \leq R \\ iA_2 \left[\frac{1}{\beta_2 r} + \frac{1}{(\beta_2 r)^2} \right] e^{-\beta_2 r} \cos\theta & r \geq R \end{cases} \quad (1.5)$$

where N_1, N_2, A_1 and A_2 are normalization constants and α_i, β_i are given by $\alpha_i = \sqrt{2m^*E_i}$ and $\beta_i = \sqrt{2m^*(V_0 - E_i)}$ with $i = 1, 2$. Matching the wave function and their derivatives at the boundary $r = R$ gives,

$$A_1 = N_1 \sin(\alpha_1 R) e^{\beta_1 R} \quad (1.6)$$

$$A_2 = -iN_2 \left(\frac{\beta_2}{\alpha_2}\right)^2 \left(\frac{\sin(\alpha_2 R) - \alpha_2 R \cos(\alpha_2 R)}{\beta_2 R + 1}\right) e^{\beta_2 R} \quad (1.7)$$

The energy Eigen values are determined by imposing the Ben Daniel and Duke boundary condition [9] is,

$$-\frac{i\hbar}{m_1^*} \frac{\partial \psi}{\partial r} (r \leq R)|_{r=R} = -\frac{i\hbar}{m_2^*} \frac{\partial \psi}{\partial r} (r \geq R)|_{r=R} \quad (1.8)$$

Using Eqs. (1.4) and (1.5) gives,

$$\frac{\partial \psi_{1s}}{\partial r} (r \leq R) = \frac{N_1 \alpha_1 \cos(\alpha_1 r)}{r} - \frac{N_1 \sin(\alpha_1 r)}{r^2}$$

$$\frac{\partial \psi_{1s}}{\partial r} (r \geq R) = \frac{-\beta_1 A_1 e^{-\beta_1 r}}{r} - \frac{A_1 e^{-\beta_1 r}}{r^2}$$

At $r = R$

$$\frac{N_1 (\alpha_1 R \cos(\alpha_1 R) - \sin(\alpha_1 R))}{R^2} = \frac{A_1 e^{-\beta_1 R} (-\beta_1 R - 1)}{R^2}$$

Substituting the value of A_1 in the above equation leads to

$$\alpha_1 R + \beta_1 R \tan(\alpha_1 R) = 0 \quad \text{for s-states} \quad (1.9)$$

$$\frac{\cot(\alpha_2 R)}{\alpha_2 R} - \frac{1}{(\alpha_2 R)^2} = \frac{1}{\beta_2 R} + \frac{1}{(\beta_2 R)^2} \quad \text{for p-states} \quad (1.10)$$

Solving these transcendental equations numerically, the confined energies E_l^n ($n = 1, 2, 3, \dots; l = 0, 1$) are obtained. For other excited states similar equations

may be obtained when $l = 2,3$. Confined energies for the first two states for various barrier heights are given in **Table 1.1**.

1.2.2 Two Electrons in a Spherical Quantum Dot

Hamiltonian of the system with the interaction of electrons is given by,

$$H = \frac{p_1^2}{2m^*} + \frac{p_2^2}{2m^*} + V_D(\vec{r}_1) + V_D(\vec{r}_2) + \frac{e^2}{\epsilon_0|\vec{r}_1 - \vec{r}_2|} \quad (1.11)$$

$$H = H_1 + H_2 + H^1, \quad \text{with } H^1 = \frac{e^2}{\epsilon_0|\vec{r}_1 - \vec{r}_2|}$$

In the two-electron system the CE is calculated using the perturbation method. Here H^1 is the perturbation term and $\epsilon_0 = 13.13$ [10] is the static dielectric constant. Two cases are considered in the present problem. In the singlet state both the electrons are in the $1s$ -state (ground state) with their reversed spins. The wave function for such case is,

$$\begin{aligned} \Psi_{1s}(\vec{r}_1, \vec{r}_2) &= \Psi_{1s}(\vec{r}_1)\Psi_{1s}(\vec{r}_2) \\ \Psi_{1s}(\vec{r}_1, \vec{r}_2) &= \begin{cases} N_1 N_2 \frac{\sin(\alpha_1 r_1)}{\alpha_1 r_1} \frac{\sin(\alpha_1 r_2)}{\alpha_1 r_2} & r_1, r_2 \leq R \\ A_1 A_2 \frac{e^{-\beta_1 r_1}}{\beta_1 r_1} \frac{e^{-\beta_1 r_2}}{\beta_1 r_2} & r_1, r_2 \geq R \end{cases} \end{aligned} \quad (1.12)$$

where N_1, N_2, A_1 and A_2 are the normalization constants. Evaluation of the CE has been made either numerical procedure or by converting the coulomb term to an integral representation involving error functions. Here, the mean value theorem is used to evaluate some of the integrals. After a lengthy and straight forward algebra,

$$\Delta E = \frac{\left(\frac{R}{2} - \frac{\sin(2\alpha R)}{4\alpha}\right) \left(\left(\frac{R}{2} - \frac{\sin(2\alpha R)}{4\alpha}\right) \left(\frac{\sqrt{2}}{R} + \frac{\sqrt{2}e^{-2\beta R}}{2\beta R}\right) + \frac{\sqrt{2}e^{-2\beta R}}{4\beta R} \left(R - \frac{\sin(2\alpha R)}{2\alpha}\right) + \frac{2\sqrt{2}e^{-4\beta R}}{8\beta^2 R} \right)}{\varepsilon \left(\left(\frac{R}{2} - \frac{\sin(2\alpha R)}{4\alpha}\right)^2 \right) + \frac{e^{-2\beta R}}{\beta} \left(\frac{R}{2} - \frac{\sin(2\alpha R)}{4\alpha}\right) + \frac{e^{-4\beta R}}{4\beta^2}} \quad (1.13)$$

The interaction energies are obtained for different dot radii for the singlet state is as shown in **Table 1.2**. In the triplet state one electron in the ground state (i.e. 1s-state) and another in the excited state (1p-state). Therefore the total spin of the system is 1 for the triplet state. In this situation the wave function of the triplet state is,

$$\Psi_A(\vec{r}_1, \vec{r}_2) = \frac{1}{\sqrt{2}} [\Psi_{1s}(\vec{r}_1)\Psi_{1p}(\vec{r}_2) - \Psi_{1s}(\vec{r}_2)\Psi_{1p}(\vec{r}_1)] \quad (1.14)$$

This is spatially anti-symmetric wave function. The Columbic interaction energy is calculated by using perturbation method. The interaction energy for the triplet state is given by,

$$\Delta E = \int \Psi_A^*(\vec{r}_1, \vec{r}_2) \frac{e^2}{\varepsilon_0 |\vec{r}_1 - \vec{r}_2|} \Psi_A(\vec{r}_1, \vec{r}_2) d\vec{r}_1 d\vec{r}_2 \quad (1.15)$$

where $\Psi_A(\vec{r}_1, \vec{r}_2)$ is given in Eq. (1.14). After a lengthy and straight forward algebra the first order correction is obtained. The normalization integral for the triplet state is

$$\int \Psi_A^*(\vec{r}_1, \vec{r}_2) \Psi_A(\vec{r}_1, \vec{r}_2) d\vec{r}_1 d\vec{r}_2 = \left(\frac{3R}{2\alpha_1^2} - \frac{3\sin(2\alpha_1 R)}{4\alpha_1^3} - \frac{3e^{-2\beta_1 R}}{2\beta_1^3} \right) \times \left(\frac{2}{R^2} \left(\frac{R}{2\alpha_2^4} - \frac{\sin(2\alpha_2 R)}{4\alpha_1^5} \right) - \frac{\sqrt{2}}{R} \left(\frac{1 - \cos(2\alpha_2 R)}{2\alpha_2^4} \right) + \frac{R}{2\alpha_2^2} + \frac{\sin(2\alpha_2 R)}{4\alpha_2^3} + \frac{e^{-2\beta_2 R}}{\beta_2^3} \left(\frac{1}{2} + \frac{1}{\sqrt{5}\beta_2 R} + \frac{1}{10\beta_2^2 R^2} \right) \right) \quad (1.16)$$

The evaluation of ΔE is tedious for triplet state. The first order correction ΔE is

$$\Delta E = \frac{(\Psi, H^1 \Psi)}{(\Psi, \Psi)} \quad (1.17)$$

The results obtained for the interaction energies are given in **Table 1.3**. The value of ΔE is given as

$$\Delta E = \frac{4\pi(A + B + C + D + E + F + G + H + I)}{3\varepsilon \int \Psi_A^*(\vec{r}_1, \vec{r}_2) \Psi_A(\vec{r}_1, \vec{r}_2) d\vec{r}_1 d\vec{r}_2} \quad (1.18)$$

where

$$A = \frac{1 - \cos(2\alpha_1 R)}{\alpha_1^2 \alpha_2^2 R^3 (\alpha_1^2 - \alpha_2^2)} \left(\frac{0.0922}{\alpha_1^2} - \frac{0.1611}{\alpha_2^2} \right) + \frac{1 - \cos(2\alpha_1 R)}{\alpha_1^3 \alpha_2^3 R^3} \left(\frac{0.177}{AD^2} - \frac{0.177}{AS^2} \right)$$

$$B = \frac{0.06488(1 - \cos(2\alpha_2 R))}{\alpha_1^2 \alpha_2^4 R^3 (\alpha_1^2 - \alpha_2^2)} + \frac{3.34847(1 - CD) + 3\sqrt{6} \cos(2\alpha_1 R) - 1}{24\sqrt{3} \alpha_1^2 \alpha_2^4 AD^2 R^3}$$

$$C = \frac{3\sqrt{6} \cos(2\alpha_1 R) - 4 - 3.34847 \cdot CS}{24\sqrt{3} \alpha_1^2 \alpha_2^4 AS^2 R^3} + \frac{0.128653}{\alpha_1^2 \alpha_2^3 R^3} \left(\frac{1 - CS}{AS^3} - \frac{1 - CD}{AD^3} \right)$$

$$D = \frac{0.010104 \cdot \cos(2\alpha_2 R) + 0.010108 \cos(2\alpha_1 R) - 0.49444}{\alpha_1^2 \alpha_2^2 R (\alpha_1^2 - \alpha_2^2)} - \frac{0.0833}{\alpha_1^2 \alpha_2^2 R^2} \left(\frac{SS}{AS^3} + \frac{SD}{AD^3} \right)$$

$$E = \frac{12 + [3\sqrt{2}(CS - 1)] - 4CS}{48\alpha_1^2 \alpha_2^2 AS^2 R} + \frac{12 + 3\sqrt{2}(CD - 1) - 4CD}{48\alpha_1^2 \alpha_2^2 AD^2 R} + \frac{0.07044}{\alpha_1^2 \alpha_2^3 R^2} \left(\frac{SD}{AD^2} + \frac{SS}{AS^2} \right)$$

$$\begin{aligned}
F &= \frac{\sin(2\alpha_1 R)}{\alpha_1^3 \alpha_2^2 R^2} \left(\frac{0.05755}{\alpha_1^2 - \alpha_2^2} - \frac{0.25\alpha_1}{\alpha_2^2 AD} - \frac{0.125}{AS^2} - \frac{0.125}{AD^2} \right) \\
&\quad + \frac{\sin(2\alpha_2 R)}{\alpha_1^2 \alpha_2^3 R^2} \left(\frac{0.44244}{\alpha_1^2 - \alpha_2^2} + \frac{0.125}{AD^2} + \frac{0.375}{AS^2} \right) \\
G &= \left(\frac{\cos(AS.R)}{3.AS} + \frac{\cos(AD.R)}{3.AD} \right) \left(\frac{\sin(AD.R)}{\alpha_1^2 \alpha_2^3 R^2 AD} - \frac{\sin(AS.R)}{\alpha_1^2 \alpha_2^3 AS.R^2} + \frac{\cos(AS.R)}{\alpha_1^2 \alpha_2^2 AS.R} \right. \\
&\quad \left. - \frac{\sin(AS.R)}{\alpha_1^2 \alpha_2^2 AS^2.R^2} + \frac{\cos(AD.R)}{\alpha_1^2 \alpha_2^2 R.AD} - \frac{\sin(AD.R)}{\alpha_1^2 \alpha_2^2 R^2 AD^2} \right) \\
H &= \left(\frac{2\sin(AD.R)}{3.\sqrt{3}.AD} - \frac{2\sin(AS.R)}{3.\sqrt{3}.AS} \right) \left(\frac{\sin(AD.R)}{\alpha_1^2 \alpha_2^4 R^3 AD} - \frac{\sin(AS.R)}{\alpha_1^2 \alpha_2^4 AS.R^3} \right. \\
&\quad \left. + \frac{\cos(AS.R)}{\alpha_1^2 \alpha_2^3 AS.R^2} - \frac{\sin(AS.R)}{\alpha_1^2 \alpha_2^3 AS^2.R^3} + \frac{\cos(AD.R)}{\alpha_1^2 \alpha_2^3 R^2.AD} - \frac{\sin(AD.R)}{\alpha_1^2 \alpha_2^3 R^3 AD^2} \right) \\
I &= \left(\frac{e^{-2.(\beta_1 + \beta_2)R}}{(\beta_1 + \beta_2)^2 \beta_1^2 \beta_2^2 .R} \right) \left(0.0211 + \frac{0.109}{\beta_2.R} + \frac{0.1}{(\beta_1 + \beta_2).R} \right. \\
&\quad \left. + \frac{0.045}{\beta_2(\beta_1 + \beta_2)R^2} \right)
\end{aligned}$$

$\int \Psi_A^*(\vec{r}_1, \vec{r}_2) \Psi_A(\vec{r}_1, \vec{r}_2) d\vec{r}_1 d\vec{r}_2$ is given in Eq. 1.16

Note: SD = sin2 (AD) R	CD = cos2 (AD) R	AD = $\alpha_1 - \alpha_2$
SS = sin2 (AS) R	CS = cos2 (AS) R	AS = $\alpha_1 + \alpha_2$

The rms values used in the present case are $\sqrt{2}/R$ for $1/r_1$ and $1/r_2$ in certain integrals.

The CE for two electrons in a GaAs dot embedded in $\text{Ga}_{1-x}\text{Al}_x\text{As}$ matrix with finite barriers is also calculated. The pressure and temperature are considered as the external perturbations. In the effective mass approximation,

the hydrostatic pressure and temperature dependent Hamiltonian is given by [10]

$$H = \frac{p_1^2}{2m^*(P,T)} + \frac{p_2^2}{2m^*(P,T)} + V_D(\vec{r}_1, P, T) + V_D(\vec{r}_2, P, T) + \frac{e^2}{\epsilon_{d,b}(P,T)|\vec{r}_1 - \vec{r}_2|} \quad (1.19)$$

The above equation can be written as,

$$H = H_1 + H_2 + H^1, \quad \text{with } H^1 = \frac{e^2}{\epsilon_{d,b}(P,T)|\vec{r}_1 - \vec{r}_2|}$$

where, $m^*(P,T)$, $\epsilon_{d,b}(P,T)$, $V_D(r_i, P, T)$ are the hydrostatic pressure and temperature dependent effective mass, dielectric constant and confining potential respectively. The two subscripts d and b stand for the potential dot (GaAs) and the potential barrier ($\text{Ga}_{1-x}\text{Al}_x\text{As}$), respectively. The values of $m^*(P,T)$ and $\epsilon_{d,b}(P,T)$ are taken from previous reports [11,12] and barrier height values are given in **Table 1.1**. P is the hydrostatic pressure in GPa and T is the absolute temperature in Kelvin. In Hamiltonian (Eq. 1.19), r_1, r_2 denote the electron positions inside the dot of radius $R(P,T)$, which also depend on pressure and temperature. The confining potential is given by,

$$V_D(r, P, T) = \begin{cases} 0 & r \leq R \\ V_0 = Q_c \Delta E_g(x, P, T) & r \geq R \end{cases} \quad (1.20)$$

where V_0 is the barrier height, Q_c is the conduction band offset parameter which is taken to be 0.6 [13]. The band gap difference depends on the concentration of Al. In the present case $\text{Ga}_{1-x}\text{Al}_x\text{As}$ is the barrier medium in

which GaAs dot is embedded. The total band gap difference [6] between the GaAs dot and the $\text{Ga}_{1-x}\text{Al}_x\text{As}$ barrier media, as a function of x , is given by,

$$\Delta E_g(x) = 1.155x + 0.37x^2 \text{ eV} \quad (1.21)$$

In the present work, when x is chosen as 0.3 and 0.4, the value of V_0 turns to be 227.88 meV and 312.72 meV respectively. The Eigen functions for the two lowest lying states within the dot are given by Eqs.(1.4) and (1.5). Using E_{1s} and E_{1p} state energies, the triplet state confined energies (Binding energy) and the CE are obtained. The effect of pressure and temperature dependent CE is found out for the triplet state using Eq.(1.13) by applying pressure and temperature dependent $1s$ and $1p$ state energies.

1.2.3 Effect of Temperature and Pressure

The hydrostatic pressure and temperature dependent conduction band effective mass of GaAs and $\text{Ga}_{1-x}\text{Al}_x\text{As}$ can be written as [14, 15]

$$\frac{m_e}{m^*(P,T)} = 1 + E \left\{ \frac{2}{E_g^\Gamma(P,T)} + (E_g^\Gamma(P,T) + \Delta_0)^{-1} \right\} \quad (1.22)$$

where $E = 7.51$ eV, is the energy related to the momentum matrix element. $\Delta_0 = 0.341$ eV is the spin-orbit splitting, m_e is the free electron mass and $E_g^\Gamma(P, T)$ is the pressure and temperature dependent energy gap for the GaAs QD at the τ -point and is given by [16,17]

$$E_g^\Gamma(P, T) = E_g^\Gamma(0, T) + bP + cP^2 \quad (1.23)$$

where $b = 1.26 \times 10^{-2} \text{eVbar}^{-1}$, $C = 3.77 \times 10^{-5} \text{eVbar}^{-2}$ and

$$E_g^\Gamma(0, T) = 1.519 - \frac{(5.405 \times 10^{-4} T^2)}{(T + 204)}$$

The effective mass of $\text{Ga}_{1-x}\text{Al}_x\text{As}$ is given by [18]

$$m_b^*(P, T) = m_d^*(P, T) + 0.083x \quad (1.24)$$

where x is the Al composition. The variation of dielectric constant with pressure and temperature is given as [19]

$$\varepsilon_{d,b}(P, T) = \begin{cases} 12.74 \exp(-1.73 \times 10^{-3} P) \exp[9.4 \times 10^{-5} (T - 75.6)] & T \leq 200\text{K} \\ 13.18 \exp(-1.73 \times 10^{-3} P) \exp[20.4 \times 10^{-5} (T - 300)] & T \geq 200\text{K} \end{cases} \quad (1.25)$$

The corresponding dielectric constant of $\text{Ga}_{1-x}\text{Al}_x\text{As}$ is given as $\varepsilon_b(P, T) = \varepsilon_d(P, T) - 3.12x$. From Eq. (1.2) the pressure and temperature dependent barrier height, the band gap difference is given by

$$\Delta E_g(x, P, T) = \Delta E_g(x) + D(x)P + G(x)T \quad (1.26)$$

where $D(x) = [-(1.3 \times 10^{-3})x] \text{eV/kbar}$ and $G(x) = [-(1.15 \times 10^{-4})x] \text{eV/K}$. The variation of dot size with pressure is given [20] by

$$R(P) = R_0(1 - 1.5082 \times 10^{-3} P) \quad (1.27)$$

In the numerical work the pressure is used in the range of 0 to 4 GPa, which corresponds to 0 to 40 Kbar. Pressures beyond 4 GPa is not considered, because of a direct to indirect band gap transition of GaAs takes place at about

4 GPa [21,22]. The Al concentration is chosen as $x \leq 0.4$, since the indirect band nature of $\text{Ga}_{1-x}\text{Al}_x\text{As}$ occurs when $x \geq 0.4$.

1.3 Results and Discussion

The confined energy for the single electron system is obtained using Eq. (1.6) and (1.7) and are listed in **Table 1.1**. Confined electron energies for 1s, 1p and triplet states for barrier concentration $x = 0.1$, $x = 0.2$ and $x = 0.3$ are given in **Table 1.1**. It is noticed that the confined energy decreases as the dot size increases. It is also observed that the p-state energy is twice as that of corresponding 1s state energies. There is no bound 1s-state for dot radii less than 40 Å and a bound 1p-state is possible if the dot radii greater than 40 Å when $x = 0.3$ and 50 Å when $x < 0.3$. These results are contrast for the QW whereas there is a bound state for every well size [6].

From **Table 1.2** it is observed that as the dot size increases, both confined and CE decreases for the single state [13, 23]. The CE and the confined energies are higher for the higher concentrations of gallium and when the two electrons are non-interacting E_{2s} is exactly twice the energy of the E_{1s} state.

From **Table 1.3** it is found that the CE is negative in the triplet state as expected. This is contrast to the singlet state energy. In the triplet state when

$x = 0.1$ it is found that as the dot size increases the CE increases and reaches maximum and then decreases. The similar result is found in the binding energies in a SQD of p-state [13]. All the other cases the correlation decreases as the dot size increases [10].

Table 1.1: Variation of confined electron energies in a spherical quantum dot

Dot Radius (Å)	Confined Energy (meV)								
	E_{1s} state			E_{1p} state [†]			$(E_{1s}+E_{1p})^*$		
	$x=0.1$	$x=0.2$	$x=0.3$	$x=0.1$	$x=0.2$	$x=0.3$	$x=0.1$	$x=0.2$	$x=0.3$
40	173.05	195.91	211.75	-	-	412.97	-	-	624.72
50	128.48	141.29	150.08	245.10	279.00	300.27	373.58	420.29	450.35
75	68.93	73.28	76.25	138.64	148.49	155.00	207.57	221.77	231.25
100	42.50	44.50	45.85	86.36	90.67	93.54	128.86	135.17	139.39
150	20.71	21.36	21.80	42.28	43.65	44.55	62.99	65.01	66.35
200	12.20	12.49	12.68	24.94	25.54	25.94	37.14	38.03	38.62
250	8.03	8.19	8.29	16.42	16.74	16.95	24.45	24.93	25.24
300	5.69	5.78	5.83	11.61	11.81	11.93	17.30	17.59	17.76
500	2.13	2.15	2.16	4.340	4.39	4.42	6.47	6.54	6.58

(Note: Dashes (-) represent the non-existence of 1p state[†] and triplet state*)

From the results of **Tables 1.2** and **1.3** it is concluded that the interaction effects are important for smaller dots and should be considered in the studies on all LDSS.

Table 1.2: Variation of two electron energies with dot radius for singlet state

Dot Radius (Å)	Sub-band Energy E_{2s} (meV) [†]			Correlation Energy (meV)			Total Confined Energy E_{2s} (meV)		
	$x = 0.1$	$x = 0.2$	$x = 0.3$	$x=0.1$	$x=0.2$	$x=0.3$	$x = 0.1$	$x = 0.2$	$x = 0.3$
20	-	762.84	947.70	-	69.83	59.58	-	832.67	1007.0
25	524.10	674.82	780.58	50.73	51.60	58.07	574.83	726.42	838.65
30	468.74	564.12	630.66	42.95	49.38	51.03	511.69	613.50	681.69
40	346.1	391.82	423.5	38.09	38.68	38.78	384.19	430.50	462.28
50	256.96	282.58	300.16	30.98	31.04	31.05	287.94	313.62	331.21
75	137.86	146.56	152.5	20.70	20.70	20.70	158.56	167.26	173.2
100	85.00	89.00	91.70	15.53	15.53	15.53	100.53	104.53	107.23
150	41.42	42.72	43.60	10.35	10.35	10.35	51.77	53.07	53.95
200	24.40	24.98	25.36	7.764	7.764	7.764	32.164	32.744	33.124
250	16.06	16.38	16.58	6.211	6.211	6.211	22.271	22.591	22.791
300	11.38	11.56	11.66	5.176	5.176	5.176	16.556	16.736	16.836
500	4.26	4.30	4.32	3.105	3.105	3.105	7.365	7.405	7.407

(Note: [†] E_{2s} corresponds to two electron non-interacting energy. Dashes represent non- existence of energy).

Table 1.3: Variation of two electron energies with dot radius for triplet state

Dot Radius (Å)	Confined Energy (meV) ($E_{1s}+E_{1p}$)			Correlation Energy (meV) ($E_{1s}+E_{1p}$)			Total Confined Energy (meV)		
	$x = 0.1$	$x = 0.2$	$x = 0.3$	$x = 0.1$	$x = 0.2$	$x = 0.3$	$x = 0.1$	$x = 0.2$	$x = 0.3$
40	-	-	624.72	-	-	-25.66	-	-	599.06
50	373.58	420.29	450.35	-7.12	-20.13	-17.69	366.46	400.16	432.66
75	207.57	221.77	231.25	-11.15	-10.44	-10.30	196.42	211.33	220.95
100	128.86	135.17	139.39	-7.72	-7.74	-7.84	121.14	127.43	131.55
150	62.99	65.01	66.35	-5.28	-5.40	-5.52	57.71	59.61	60.83
200	37.14	38.03	38.62	-4.11	-4.21	-4.27	33.03	33.82	34.35
250	24.45	24.93	25.24	-3.39	-3.48	-3.52	21.06	21.45	21.72
300	17.30	17.59	17.76	-2.94	-2.96	-2.96	14.36	14.63	14.80
500	6.47	6.54	6.58	-1.87	-1.86	-1.83	4.60	4.68	4.75

(Note: Dashes represent non-existence of bound state)

When compared the values of total confined energies from **Table 1.2** and **1.3** it is found that the singlet state is lower than that of triplet state energies up to 200 Å above which triplet state energy is lower than singlet state energy. The similar crossing of singlet and triplet state energies for larger

dot radii is found by Szafran et al. who have considered an infinite barrier well with parabolic confinement, which is attributed due to numerical inaccuracies [9]. As R tends to infinity the $1s$ and $1p$ state energies are degenerate, whether a singlet state is favoured or a triplet state? By Hund's rule, a triplet state is expected without violating the Pauli principle.

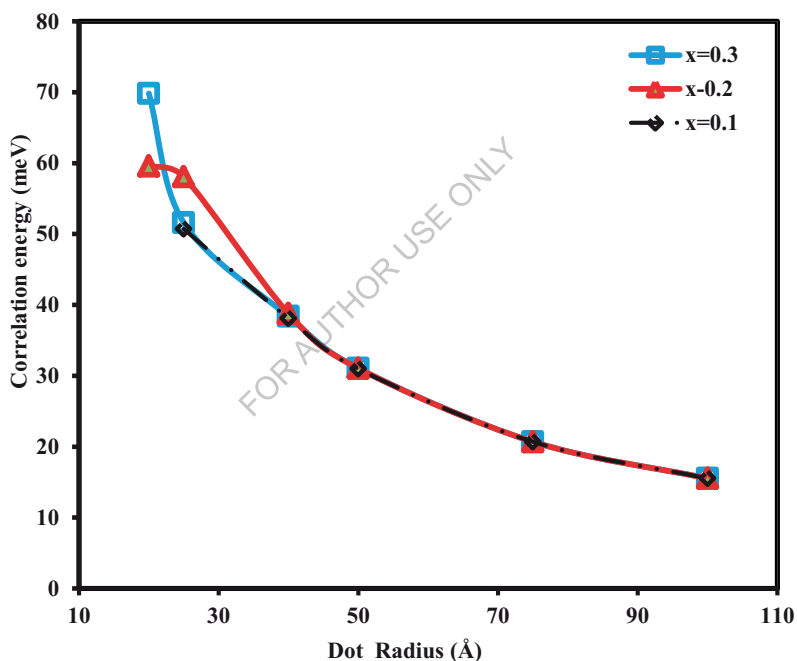


Figure 1.1: Correlation energy of singlet state (2S state) of a spherical quantum dot as a function of dot radius and different values of concentration

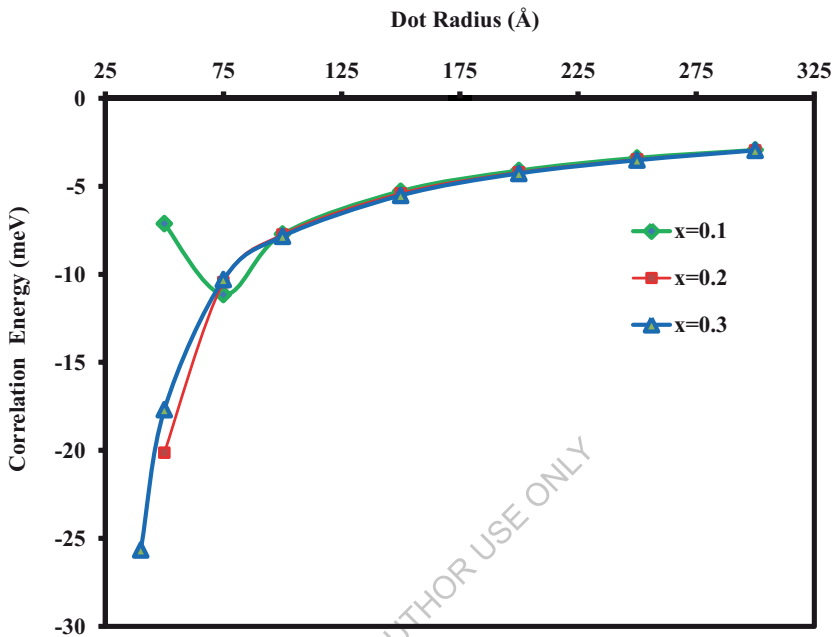


Figure 1.2: Correlation energy of triplet state of a spherical quantum dot as a function of dot radius and different values of concentration

Figure 1.2 displays the CE of triplet state of a SQD as a function of dot radius and different values of x. Here the CE is negative due to the attractive

nature of the electrons and exchange of interaction. This correlation arises due to anti-symmetric nature of wave function.

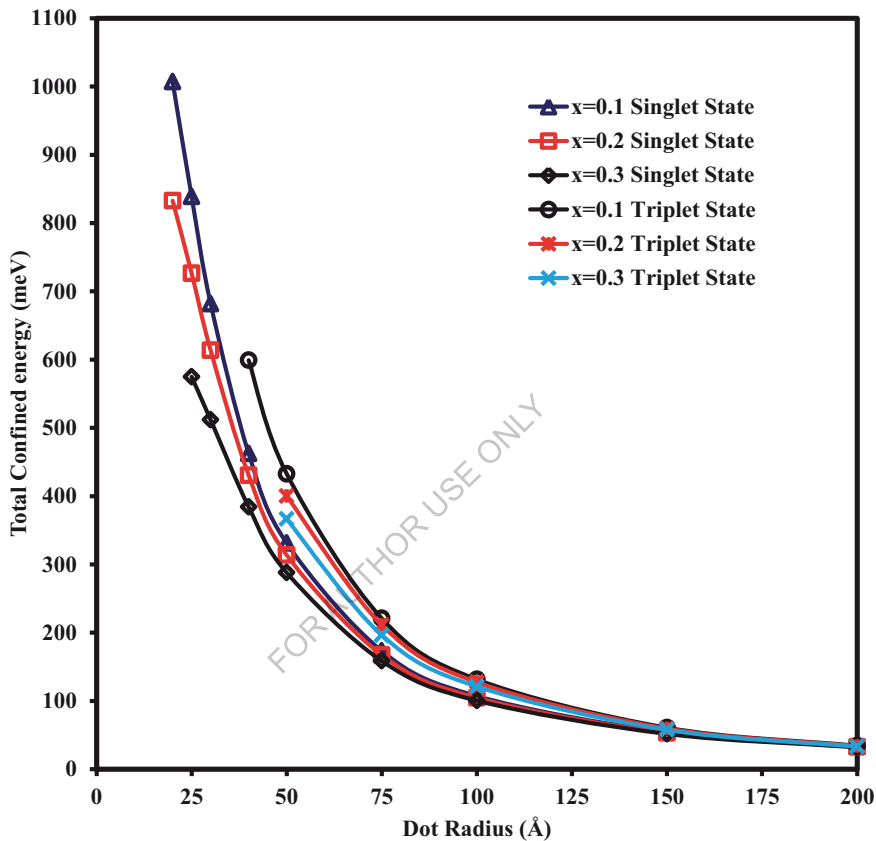


Figure 1.3: Total confined energy of singlet state and triplet state of a spherical quantum dot as a function of dot radius and different values of concentration

When $x = 0.1$ the CE increases up to the dot radii of 75 Å and then decreases. Below 50 Å there is no bound state for these cases. The similar results also have been seen in Ref. [18] in which binding energy reaches the maximum value for the dot radii of 75 Å to the p - state.

Figure 1.3 represents the variation of total confined energy of singlet and triplet states of a SQD as a function of dot radius with different concentrations. It is found that the total confined energy decreases as the dot radius increases and the energy of singlet state is lower than that of triplet state energies up to 200 Å in support of the general principle that the energy of the system should be lowest. The above result is in well agreement with quantum Monte Carlo effective mass approximation [25] and singlet-triplet splitting for the two-electron system in anisotropic harmonic-oscillator potential as a function of QD [2], in which the singlet state energy is lower than of triplet state for narrow dots. For larger dot percentage the confinement also decreases and it seems to be more or less same for both the states. For larger dot radii the total confined energy approaches the bulk value of GaAs for singlet and triplet at all the concentrations.

Figure 1.4 presents the variation of total confined energy with gallium concentration for dot size of 50 Å and 150 Å respectively. It has been clear

that the gallium concentration increases, the total confined energy also increases linearly for the dot radii of 50 Å.

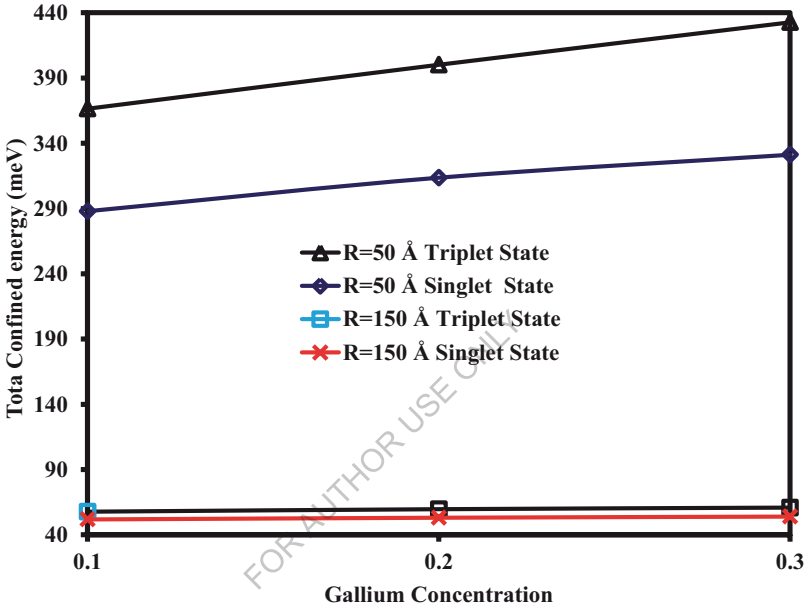


Figure 1.4: Variation of confined energy verses gallium concentration in the finite barrier model for dot radius 50 Å and 150 Å respectively

Thus the slope of the curve also depends on gallium concentration. Like other systems when GaAs dot is embedded in $\text{Ga}_x\text{In}_{1-x}\text{Sb}$ matrix, the dielectric mismatch becomes insignificant, especially when x is small. When compared

the total confined energy of gallium at the concentration of 0.1, $x = 0.3$ exhibit larger confined energy. Thus gallium concentrations are also important for the SQD. The enhancement of the binding energies, phonon energies and electron phonon energies are well known in literature [26]. The CE and the confined energy enhanced the total confined energy of the SQD.

Table 1.4: Variation of the effective mass and dielectric constant for the GaAs and Ga_{1-x}Al_xAs at aluminium composition, $x = 0.4$

T(K)	Effective mass		Dielectric constant		Barrier Height (meV)
	GaAs	Ga _{1-x} Al _x As	GaAs	Ga _{1-x} Al _x As	
0	0.066998	0.100	12.65	11.402	312.72
100	0.066305	0.100	12.77	11.521	309.96
200	0.064908	0.098	12.91	11.642	307.20
300	0.063221	0.096	13.18	11.764	304.44
400	0.061382	0.095	13.45	11.886	301.68
500	0.059451	0.093	13.73	12.011	298.92
600	0.057459	0.091	14.01	12.136	296.16

The effect of external perturbation like temperature and pressure on various parameters used in the calculation and their values at various temperatures are given in **Table 1.4**. From this, it is found that the increase in temperature will decrease the values of both the effective mass and the barrier height and increase the dielectric constant of GaAs and $\text{Ga}_{1-x}\text{Al}_x\text{As}$.

Table 1.5: Temperature and pressure dependent correlation energies in a spherical quantum dot

Pressure (GPa)	Correlation Energy (meV)							
	T = 0K				T = 600K			
	R=50Å	R=65Å	R=100Å	R=150Å	R=50Å	R=65Å	R=100Å	R=150Å
0	-43.99	-24.56	-15.09	-9.63	-40.02	-22.24	-13.99	-8.79
1	-44.50	-24.84	-15.17	-9.69	-41.13	-21.34	-14.37	-8.94
2	-44.94	-25.57	-15.27	-9.77	-41.79	-23.45	-14.65	-9.38
3	-45.67	-25.71	-15.36	-9.89	-42.67	-23.98	-14.93	-9.65

Table 1.5 explains the temperature and pressure dependent correlation energies in a SQD. It is found that the CE decreases as the dot size increases, a feature that is well known in literature [7, 10]. The CE decreases as the temperature increases and it increases as the pressure increases. Also it is

observed that the CE is negative as expected for the triplet state. This is a consequence of the exchange interaction in the triplet state. This interaction arises because of the anti-symmetric nature of the wave functions Eq. (1.14).

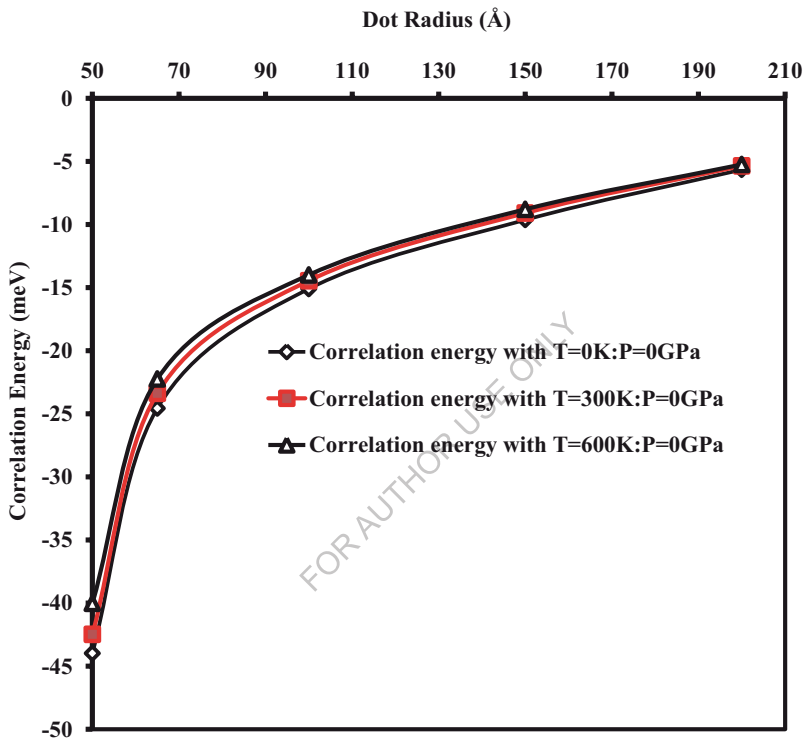


Figure 1.5: Variation of correlation energy with different dot radii for different temperatures $T = 300$ K and 600 K at 0 GPa when $x = 0.4$

Figure 1.5 shows the variation of CE with the dot radius for various temperatures at $T = 0\text{K}$, 300K and 600K at 0GPa pressure. It is found that the CE decreases with the dot radii for all temperatures. It also decreases due to increase in temperature since the values of the effective mass decreases. As a result the increased effective Bohr radius lead the potential barrier height to decrease, and for larger dot size it shows 3D behaviour. For the smaller dot radii there is 5% decrease in correlation due to application of temperature. It is found that the CE is higher for smaller dot size of higher aluminium concentration. It approaches to zero as the dot radius tends to infinity. Also there is no CE for dot radii less than 50\AA , because no bound $1p$ state is possible since the barrier height itself is 312.72 meV when $x = 0.4$.

Figure 1.6 shows the variation of CE with different dot radius for the temperature $T = 600\text{K}$ with and without the pressure. It is noticed that the hydrostatic pressure increases the CE for all the dot sizes for the given temperature. The physical reason of this behavior is that as the pressure goes up, the wave functions are very confined for the dot and the effective mass and dielectric constant increases. For the smaller dot radii there is 4.5% increase in correlation due to application of pressure. Thus the simultaneous application of pressure and temperature, it is observed that the CE decreases for all dot sizes.

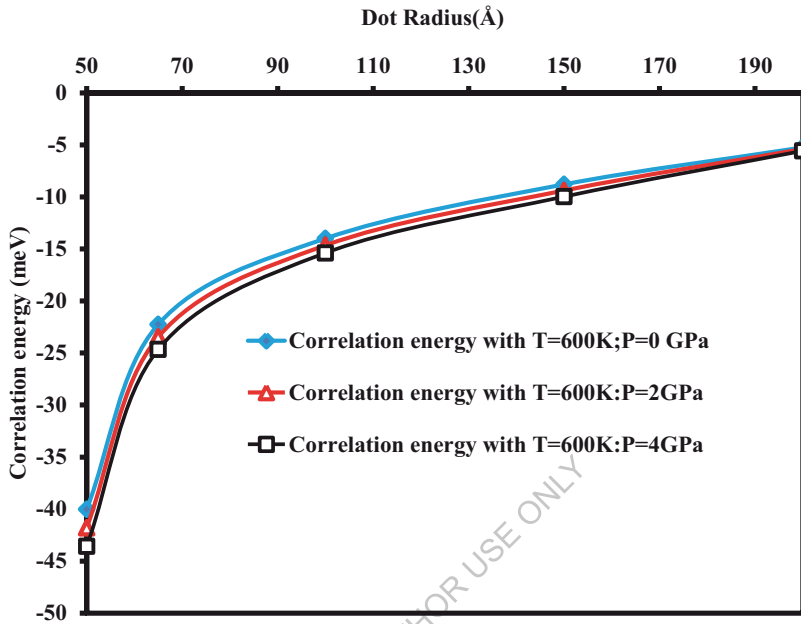


Figure 1.6: Variation of correlation energy with different dot radii for the temperature $T = 600$ K with and without the pressure when $x = 0.4$

Figure 1.7 presents the variation of CE with different dot radius for the temperature $T = 600$ K and $P = 0$ GPa for the singlet and triplet state. Here the value of aluminium concentration is considered as $x = 0.3$, in order to compare with the reference singlet state energies [27]. It is observed that the triplet state

energies are negative and it is almost equal to the magnitude of singlet state energies but positive [7]. In the singlet state there is no exchange interaction among the electrons of opposite spin orientations. Thus the CE is repulsive. However in the triplet state the exchange interaction is attractive which favors the parallel arrangement of spins via Hund’s rule as in ferromagnetism. There is no CE for triplet state when the dot radii less than 65 Å, because no bound 1p state is possible since the barrier height itself is 227.88 meV when $x = 0.3$.

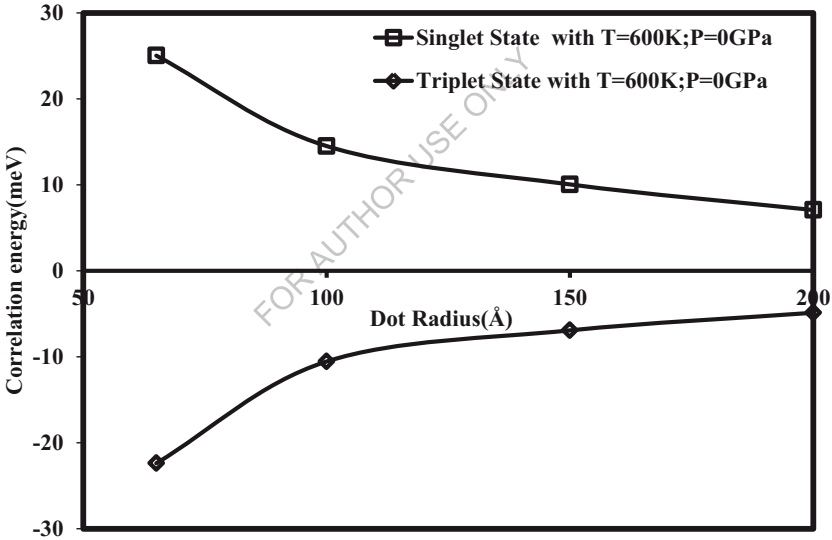


Figure 1.7: Variation of correlation energy with different dot radii for the temperature $T = 600$ K and $P = 0$ GPa when $x = 0.3$

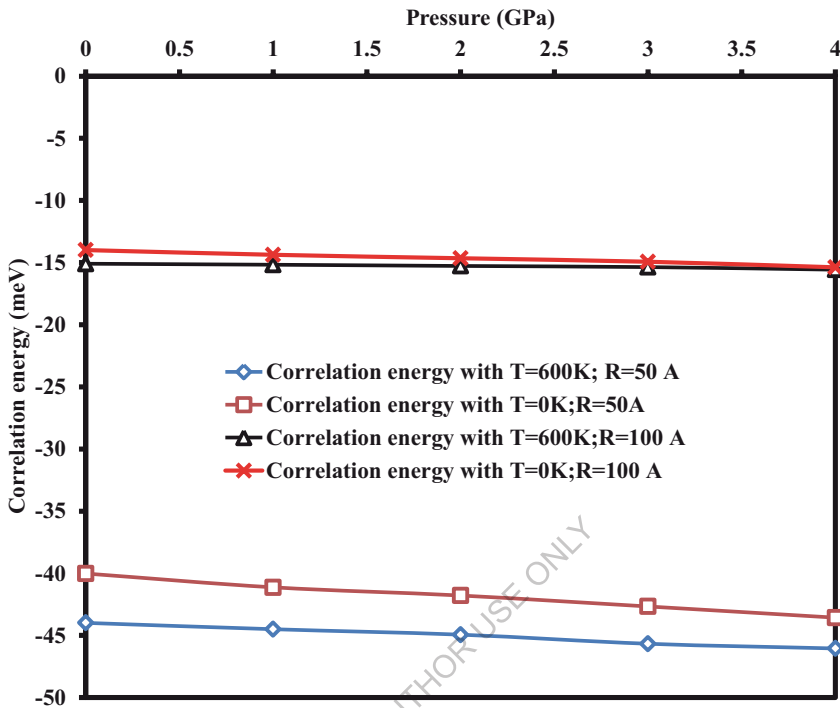


Figure 1.8: Variation of correlation energy versus pressure with different temperatures ($T = 0\text{K}$ and 600K) and dot radii ($R = 50\text{ \AA}$ and 100 \AA)

In **Figure 1.8** the variation of CE with the applied pressure at different temperatures ($T = 0\text{K}$ and 600K) and dot radii ($R = 50\text{ \AA}$ and 100 \AA) have been presented. The correlation energies linearly increases with the pressure. This is due to the increment of the effective mass, dielectric constant and

barrier height. For smaller dot radius the variation of CE is higher as compare to the larger dot radii. The hydrostatic pressure and temperature dependence exciton binding energy inside a cylindrical QD is studied by Nagwa Elmeshad et al. and they found that the exciton binding energy increased as the hydrostatic pressure increases and in contrast here it is decreased when the dot size increases [28]. These results are in agreement with our results, since the wannier excitons behave very much like an atomic system (QD).

In **Figure 1.9** the variation of CE as a function of temperature with different pressures ($P = 0$ and 4 GPa) and dot radii ($R = 50$ and 100 Å) are displayed. The CE is linearly decreases with the temperature. This is due to the increased values in effective mass, dielectric constant and barrier height. Liang et al. found that the ground state binding energy of the neutral donor in a QD increased as the hydrostatic pressure increases [29]. The physical origin of the result is related to the effect of the existence of the Coulomb repulsion in an exciton - donor complex system.

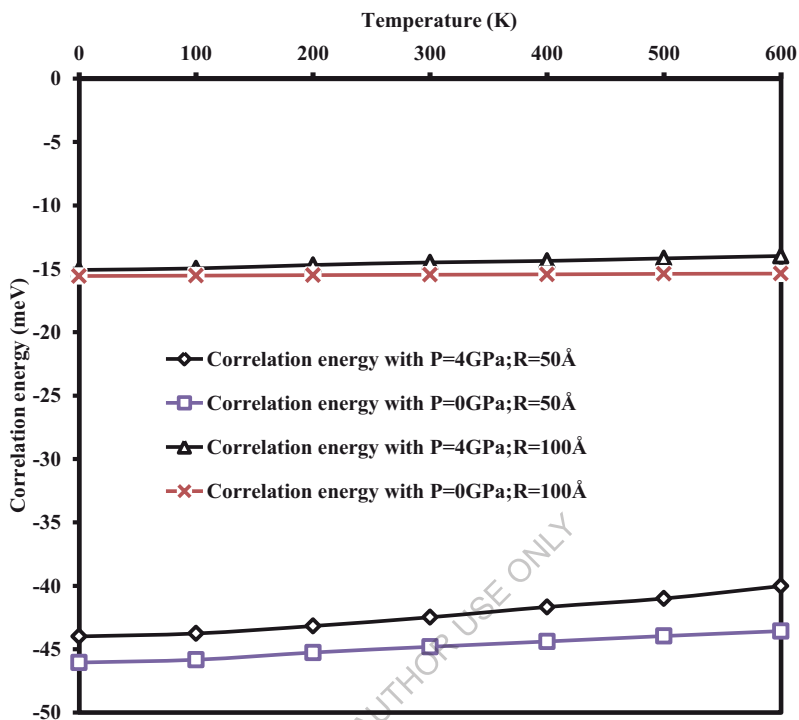


Figure 1.9: Variation of correlation energy as a function of temperature with different pressures ($P = 0$ and 4 GPa) and dot radii ($R = 50 \text{ \AA}$ and 100 \AA).

Moreover, it is observed that the influence of pressure on the CE is more obvious than temperature which is also due to columbic repulsion. The important result that emerges from the present chapter is that the pressure and temperature effects are important for smaller dots and should be consider in the studies of LDSS.

1. 4 Conclusion

In the present chapter the confined energy of two electrons in a spherical QD and its interaction effects with external perturbations are investigated. All the calculations have been carried out with finite models. The confined energy and its interaction effects of singlet and triplet state of GaAs/Ga_xIn_{1-x}Sb are discussed. The combined effects of hydrostatic pressure and temperature on the CE in the triplet state of GaAs/Ga_{1-x}Al_xAs for a two electron SQD are also discussed. The perturbation approach is used within the effective mass approximation. The interaction energy (Correlation Energy) is computed for GaAs/Ga_xIn_{1-x}Sb and GaAs/Ga_{1-x}Al_xAs as a function of the dot size. Results are presented for the SQD with square well confinement corresponding to different values of x . The important conclusions that emerged from this chapter are:

- ✓ The confined and correlation energies are decreased as the dot size increases.
- ✓ Correlation energies are important for smaller dot size.
- ✓ Correlation energy is negative for triplet state which reflecting the exchange interaction and it contribute 4 - 8% decrement in total confined energy to the narrow dots.

- ✓ Correlation Energy is positive for singlet state and it contribute 6-10% increment in total confined energy to the narrow dots.
- ✓ In the triplet state it increases with increase in pressure and it further decreases due to the application of temperature and it contributes 10% decrement in total confined energy to the narrow dots.
- ✓ The singlet state and triplet state CE and total confined energy tends to zero as dot radius tends to infinity.
- ✓ The concentration of impurity also important while determining the correlation and confined energies. The effect of hydrostatic pressure increases the correlation energy may be used to tune the output of optoelectronic devices without modifying the physical size of the QD. The effect of high temperatures is quite significant in small dot radii due to thermal broadening in the mixed quantum state.

References

- [1] P. Harrison, Quantum wells, wires and dots: *Theoretical and Computational Physics of Semiconductor Nanostructures* Wiley third edition (2010).
- [2] B. Szafran, J. Adamowski and S. Bednarek, *Physica E* 5 (2000) 185.
- [3] G. Cantele, D. Ninno and G. Iadonisi, *Phys. Rev. B* 64 (2001) 125325.
- [4] L. He, G. Bester and A. Zunger, *Phys. Rev. B* 72 (2005) 195307.
- [5] G. Parasandolo *et al.* *Phys. Rev. B* 68 (2003) 245318.
- [6] V. V. Mitin, V. A. Kochelap and M. A. Strosio, *Micro Electronics and Optoelectronics*, Cambridge: Cambridge University Press, 122 (1999).
- [7] A. R. Jeice and K. Navaneethakrishnan, *Braz. J. Phys.* 39 (2009) 526.
- [8] T. Kumar, P. Ramesh and S. D. G. Ram, *Digest J. Nanomater. Biostruct.* 6 (2011) 683.
- [9] Y. Li, O. Voskoboynikov, J. L. Liu, C. P. Lee and S. M. Sze, *Nanotech.* 1 (2001) 562.
- [10] A. Sivakami and K. Navaneethakrishnan, *Physica E* 40 (2008) 649.
- [11] A. M. Elabasy, *Physica Scripta* 59 (1999) 328.
- [12] G. Samara, *Phys. Rev. B* 27 (1983) 3494.
- [13] R. S. Daries Bella and K. Navaneethakrishnan, *Solid State Commun.* 130 (2004) 773.

- [14] H. J. Ehrenreich, *J. Appl. Phys.* 32 (1961) 2155.
- [15] E. Kasapoglu, *Physics Letters A* 373 (2008) 140.
- [16] B. Welber, M. Cardona, C. K. Kim and S. Rodriguez, *Phys. Rev. B* 12 (1975) 5729.
- [17] D. E. Aspnes, *Phys. Rev. B* 14 (1976) 53319.
- [18] A. Sivakami and V. Gayathri, *Superlat. Microstruct.* 58 (2013) 218.
- [19] A. John Peter and K. Navaneethakrishnan, *Superlat. Microstruct.* 43 (2008) 63.
- [20] S. Adachi, *GaAs and Related Materials*, first ed., *World Scientific*, Singapore, 1994.
- [21] Sr. Gerardin Jayam and K. Navaneethakrishnan, *Solid State Commun.* 126 (2003) 681.
- [22] S. Adachi, *J. Appl. Phys.* 58 (1985) R1.
- [23] A. Sivakami and M. Mahandran, *Superlatt. Microstruct.* 47 (2010) 530.
- [24] A. J. Peter and S. S. Kumar, *Physica E* 41 (2008) 138.
- [25] C. Yannouleas and U. Landman, *J. Phys.: Condens. Matter* 14 (2002) 1591.
- [26] B. K. Ridley, *Electronics and Phonons in semiconductor Multilayers* Cambridge: Cambridge University Press (1997).
- [27] A. Sivakami and M. Mahendran, *Physica B* 405 (2010) 1403.

- [28] N.Elmashad, H. Abdelhamid, H Hassanein, S. Abdelmola and S. Said,
Chinese J. Phys. 47 (2009) 1.
- [29] S. J. Liang and W. F. Xie, *Eur. Phys. J. B* 81 (2011) 79.

FOR AUTHOR USE ONLY

FOR AUTHOR USE ONLY

FOR AUTHOR USE ONLY

FOR AUTHOR USE ONLY

**More
Books!** 



yes
I want morebooks!

Buy your books fast and straightforward online - at one of the world's fastest growing online book stores! Environmentally sound due to Print-on-Demand technologies.


Buy your books online at
www.get-morebooks.com

Kaufen Sie Ihre Bücher schnell und unkompliziert online – auf einer der am schnellsten wachsenden Buchhandelsplattformen weltweit!
Dank Print-On-Demand umwelt- und ressourcenschonend produziert.

Bücher schneller online kaufen
www.morebooks.de

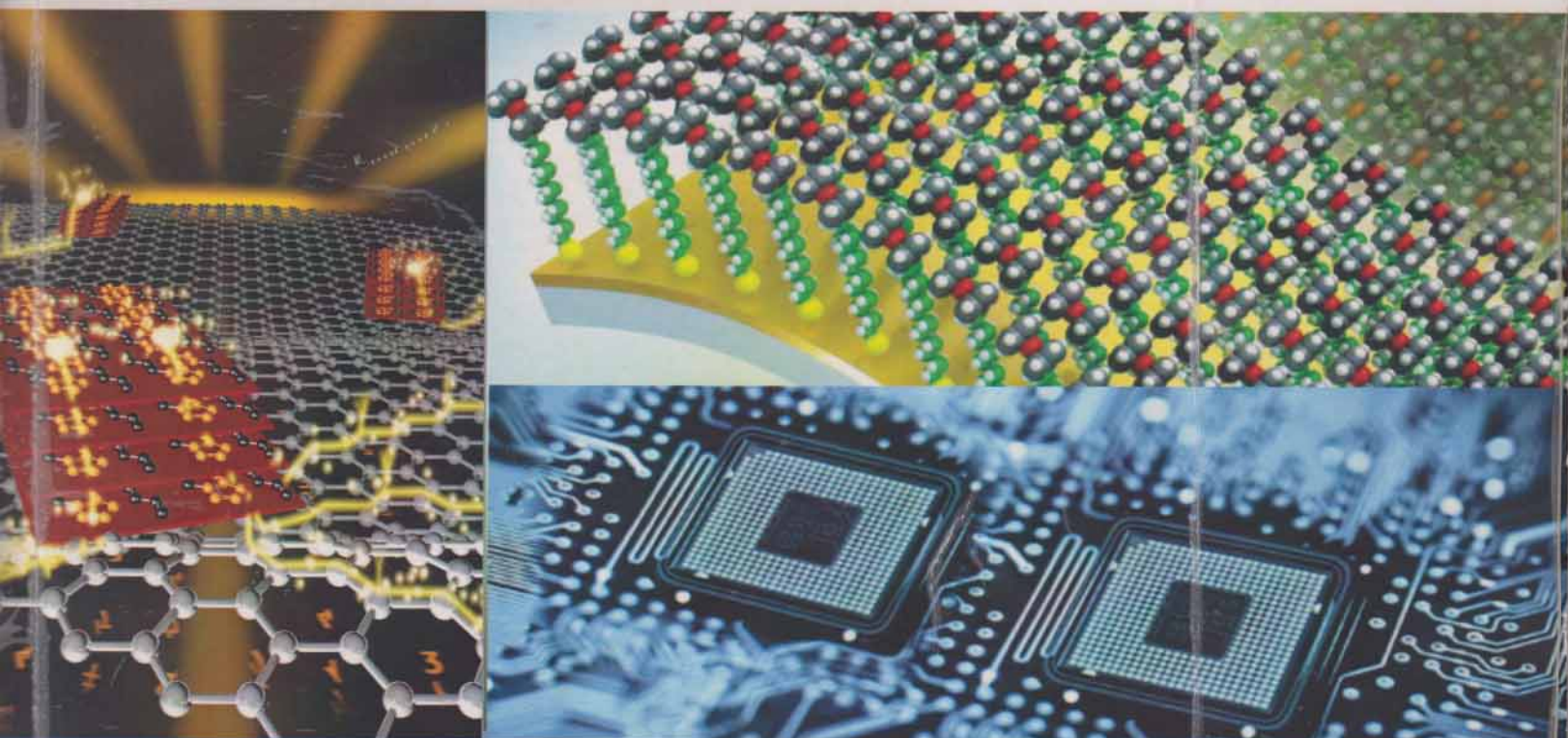
OmniScriptum Marketing DEU GmbH
Bahnhofstr. 28
D - 66111 Saarbrücken
Telefax: +49 681 93 81 567-9

info@omniscrptum.com
www.omniscrptum.com

OMNI Scriptum 

FOR AUTHOR USE ONLY

**Proceedings of the
International Workshop on
Advanced Functional Materials and Devices
8 - 12 January 2017**



Organised by
Department of Physics & Department of Chemistry
Manonmaniam Sundaranar University
Tirunelveli



A functional deep UV nonlinear optical crystal Sulphamic acid admixed Phosphoric acid (SAPA): Synthesis, growth and Characterization

Y.Samson^{1,3}, S. Anbarasu², M. Ambrose Rajkumar³ D. Prema Anand^{3*}

¹Department of Physics, Annai Velankanni College, Tholayavattam- 629157, Tamilnadu, India

²Department of Physics, Loyola College of Arts & Science, Mettala-Oilpatty, Rasipuram (Tk.), Namakkal (Dt.)-636202, Tamilnadu, India

³Physics Research Centre, Department of Physics, St. Xavier's College (Autonomous), Palayamkottai-627002, Tamilnadu, India.

* Corresponding Author(s): devarajanpremanand@gmail.com (D. Prem Anand)

Abstract:

An advanced optical functional DUVNLO Sulphamic acid admixed Phosphoric acid (SAPA) crystal was synthesized and grown from aqueous solution by slow evaporation technique at room temperature. SAPA crystallizes in Tetragonal P. It exhibits a short absorption edge closer to 200 nm in UV spectrum. SHG efficiency is measured as 0.59 times of KDP.

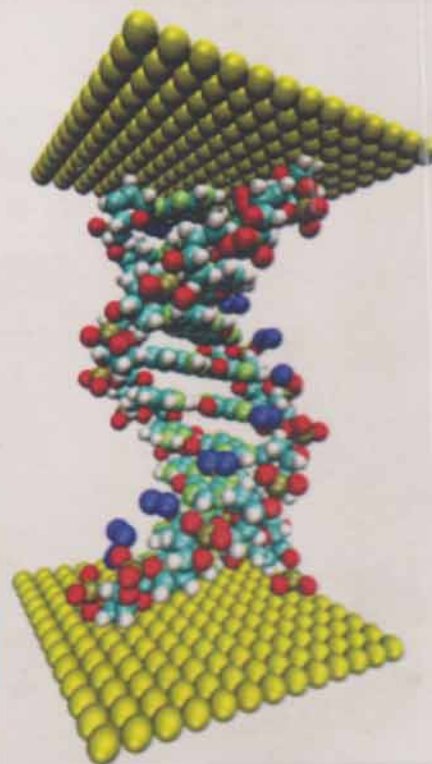
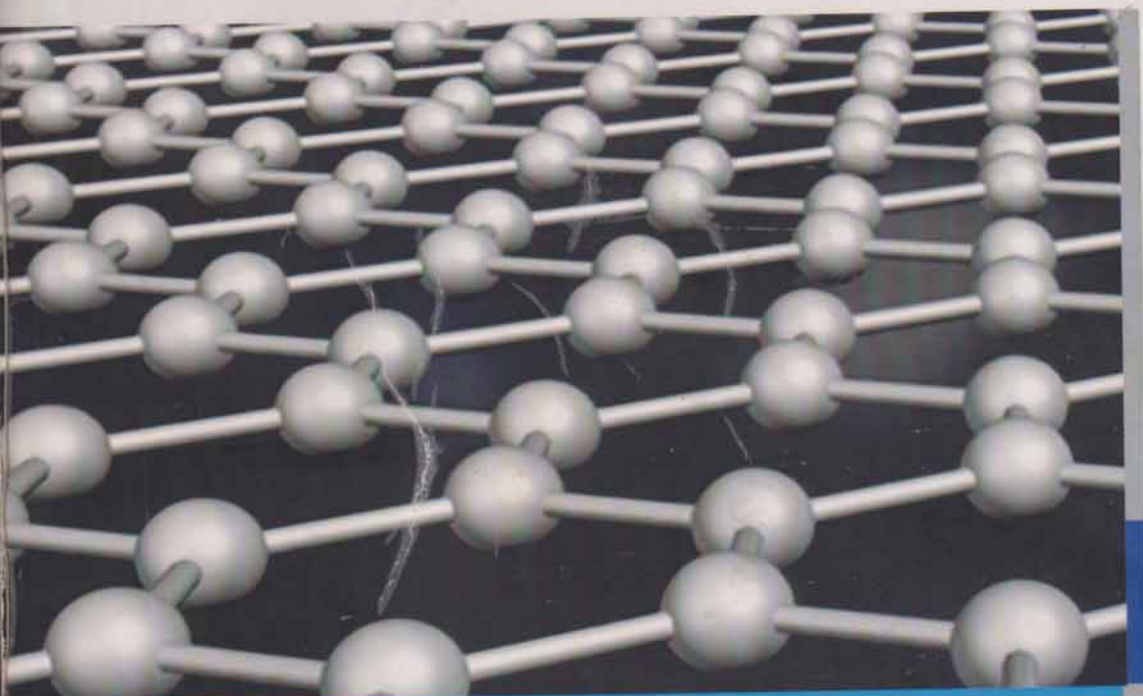
Key-words: SAPA, slow evaporation technique, deep UVNLO, SHG

Introduction:

Global concern has been converged on functional nonlinear optical (NLO) materials which charted the path to harvest energy hugely profitable in laser micromachining, photochemistry, photoemission spectroscopy, lithography, fluorescence detection, surface-enhanced Raman scattering, communication, surgery, atto-second pulse generation etc^[1,2]. Functional NLO materials are capable of functioning to control and alter electromagnetic radiation in ultraviolet (UV), visible, infrared (IR) spectral region. Their optical character as a function of incident wavelength and frequency depends on inherent properties like structure, thermal, chemical stabilities and on external fields applied^[3]. Deep UV (DVU) NLO crystals are optically functioning to transmit the light of wavelengths lesser than 200 nm in UV region by cascaded frequency conversion. They have been fabricated by fusing borates, borate-fluorides, carbonate-fluorides and phosphates with various metal units (alkali, alkaline earth, transition elements). The challenges of decomposing nature of carbonates, hard growth habit and toxicity of berilyium borates, cost effective melt growth techniques were identified. In contrast, phosphate endowed with long chain geometry, good thermal, chemical stabilities, enhanced SHG, easily grown nature circumvent the aforesaid problems. It leverages us to design Sulphamic acid admixture Phosphoric acid (SAPA) optical functional crystal for desired DUVNLO applications.

Experimental Techniques and Material Characterization:

SAPA was obtained from an aqueous solution containing sulphamic acid admixed with phosphoric acid in equimolar ratio was stirred for 3 hrs and allowed for slow evaporation at room temperature. Centimeter sized crystal was harvested within 28-30 days. Crystallographic data was collected from Bruker Kappa APEXII Single Crystal X-ray Diffractometer. The crystalline phases were



Organised by
Department of Physics & Department of Chemistry
Manonmaniam Sundaranar University
Tirunelveli. Tamil Nadu, INDIA.

Sponsored by



ISSN 978-93-81402-38-2



9 789381 402382

CYBA publication Series - IV

Biotechnology for Sustainable Development

Editors

Dr. V. A. J. Huxley

Dr. S. Prakash

Dr. J. M. Sasi Premila

Dr. T.Suresh

BIOTECHNOLOGY TOWARDS SUSTAINABLE AGRICULTURE AND ENVIRONMENT

Dr.J.M.SASI PREMILA

Asst.Professor ,Department of Biotechnology

Annai Velankanni College, Tholayavattam.

Abstract:

Biotechnology is a frontline technologies today being developed and used to understand and manipulate biological molecules for applications in medical, agricultural, industrial and environmental sectors of the national economy. Biotechnology is safe, effective and widely used by more than 18 million farmers around the world. It is a proven tool that has successfully improved crop productivity for growers around the world since 1995, resulting in an abundant and affordable food supply. Various studies have shown the safety of the technology to human beings, animals and the environment. Increasing global food production within existing land area and the use of modern plant breeding methods have enhanced increased production of crops like legumes to improve soil structure, organic matter and fertility. These lead to conservation of bioresources and prevent soil erosion. The aim of this review is to emphasize the importance of Biotechnology towards attaining a safe and sustainable environment for increased global agricultural production.

Key words: Biotechnology, Bioresources, agricultural production,

Introduction:

Biotechnology can be defined as any technological application that uses biological systems, living organisms or derivatives to make or modify products or processes for specific use (UNCBD, 1992). Traditionally, micro-organisms have been deliberately used to produce beverages and fermented foods (Olatunji, 2007). Environmental biotechnology is the application of biotechnology to the study of natural environment. Environmental Biotechnology as the development, use and regulation of

About CYBA

Cape Young Biologists Association (CYBA) was established in 2006 by the bio researchers of Kanyakumari dist, amilnadu and registered under Govt. Tamilnadu. The members of organization are more than 100 young scientists and researchers from universities and scientific institutions. Our mission is to consolidate young professionals from different fields of biology, to realize their ideas, and to implement clean, transparent, devoted research in biology and nature conservation oriented projects. Our activities are also directed to expand youth participation towards society development.



Published by



Hari Krish Publication

ISBN 978-93-80819-11-2



9 789380 819112 >

Dr. M. Josephine Rani is an Associate Professor of Commerce, Annai Velankanni College, Thalayavattam. She obtained her Master degree in Commerce from St. Joseph's College, (Autonomous) Palayambottai, Master of Business Administration (MBA) from Tamil Nadu Open University and Doctoral Degree (Ph.D) from Manonmaniam Sundarman University, Tirunelveli. She has more than 10 years teaching experience in US as well as 10 and she had produced eight M.Phil students. She is a recognized research guide in Manonmaniam Sundarman University, Tirunelveli. She has published many articles in various approved research journals. She had attended and organized national as well as international conferences.

B-DIGEST Publications

16/7, Deshasthappan Street,
Hosurpet, Kanyakumari District,
TamilNadu - 626 001. www.bdigest.in
e-mail: bdigestpublications@gmail.com



IMPORT & EXPORT PROCEDURES



Dr. M. Josephine Rani

Reproduction or translation of any part of this book by any means without prior permission from the publisher is unlawful. Requests for permission or further information should be addressed to the publisher.

Rs. : 300/-

ISBN : 978-93-84734-56-5

Published by
B-DIGEST Publications
18/7, Devasahayam Stree,
Nagercoil, Kanyakumari District,
Tamilnadu - 629 001. www.bdigest.in
e-mail : bdigestpublications@gmail.com
Mobile : +91 94 88 88 84 00

Printed by
MeraPrinters
Mullanganavilai & P.O.
Ph : 04651-267344, 9345699988

CONTENTS

1. INTERNATIONAL TRADE	1
2. BALANCE OF TRADE	29
3. EXPORT PROCEDURES	54
4. IMPORT PROCEDURE	84
5. EXPORT PROMOTION	120
6. MODEL QUESTION PAPER	146